Miniemulsion Copolymerization of Methyl Methacrylate and Butyl Acrylate by Ultrasonic Initiation

Melanie A. Bradley,[†] Stuart W. Prescott,[†] Harold A. S. Schoonbrood,[‡] Katharina Landfester,[§] and Franz Grieser*[,†]

Particulate Fluids Processing Centre, School of Chemistry, The University of Melbourne, Victoria 3010, Australia; Wacker Chemicals Australia, Unit 18/20 Duerdin St, Clayton North Victoria 3168, Australia; and Max-Planck Institute for Colloids and Interfaces, Forschungscampus Golm, 14424 Potsdam, Germany

Received December 21, 2004; Revised Manuscript Received May 19, 2005

ABSTRACT: The ultrasonically initiated batch miniemulsion copolymerizations of methyl methacrylate (MMA) and butyl acrylate (BA) are studied at different MMA:BA ratios (including homopolymerizations), and the physical properties and chemical composition of the polymers formed are investigated. Trends in the evolution of the particle number are rationalized with reference to the mechanical properties of the polymer particles, with the number concentration of the softer, BA-rich particles reducing with continued sonication. Molecular weight data are consistent with high radical fluxes entering the particles, with the radical entry frequency calculated from the peroxide yield in a model system to be $\sim 1.5 \times 10^{-2}$ s^{-1}. To within experimental uncertainty, the copolymer composition is found to be consistent with the terminal model for propagation reactions and previously published reactivity ratios; hence, it is concluded that ultrasound has little effect on the propagation step in a free-radical polymerization process. The results obtained also support a miniemulsion polymerization pathway for sonochemically synthesized latex particles.

Introduction

The effects of ultrasound on a chemical process are both mechanical and chemical in origin, although mechanistic understanding of sonochemical reactions has only been developed relatively recently.[1] Irradiation of liquids with ultrasound causes enhanced mass transport, emulsification, and bulk thermal heating—effects that have been exploited in the preparation of miniemulsion polymerizations.[2,3]

The chemical effects of ultrasound derive primarily from acoustic cavitation involving the formation, growth, and implosive collapse of bubbles. At an ultrasound frequency of 20 kHz, the local temperature of the collapsed microbubble in an aqueous solution is ~4300 K.[4] These high temperatures lead to the homolysis of water within the bubbles, creating $^{\bullet}$OH and H$^{\bullet}$ radicals,[5] which have previously been shown to initiate polymerization with a variety of monomers.[6]

Miniemulsions consist of stable nanometer-sized droplets, and particle formation in the polymerization of such systems is by droplet nucleation.[7] Droplet stability is typically maintained by the use of a costabilizer/surfactant system; added ionic or nonionic surfactant stabilizes the droplets against collisional growth, while an added costabilizer (a hydrophobe such as hexadecane) stabilizes against Ostwald ripening.[2] Recent advances in miniemulsion polymerization have demonstrated that with a suitable choice of stabilizing group[8] or with constant agitation[9] the costabilizer may not be necessary for a miniemulsion polymerization to be undertaken.

The free radicals produced during cavitation are used here in the ultrasonically initiated miniemulsion polymerization of methyl methacrylate. Previous reports of ultrasonically initiated dispersed-phase polymerization indicate that monomer conversion at ambient temperature is possible.[9−14] It is interesting that miniemulsion polymerizations described elsewhere have frequently made use of ultrasound for agitation, but *not* for initiation, with chemical initiators being added to the reaction after a period of sonication.[2] Moreover, the same irradiation frequency and power (even the same make and model sonicator) have been used. The key differences between this work and studies of "classical" miniemulsions for which ultrasound has been only for agitation are that here (i) argon sparging is used to increase the cavitation temperature (hence, increasing the radical flux), as compared with, for example, nitrogen; (ii) oxygen is excluded during sonication; (iii) the temperature is maintained at ~25 °C, whereas during many (but not all) conventional miniemulsion preparations temperature escalations are quite common, hence the radical flux here is higher (increasing the water temperature reduces the cavitation temperature, lowering the chemical yield of radicals[15]); (iv) the droplets are produced in the absence of a costabilizer, are unstable, and require continual agitation until polymerization commences within them (balancing Ostwald ripening), whereas miniemulsions may normally be stored for some time before use.

In this work, the miniemulsion copolymerization and homopolymerization of methyl methacrylate and butyl acrylate are studied, with initiating radicals derived from an ultrasonic field. The physical properties of these copolymers are compared to conventionally produced emulsion copolymers, and the compositions of the copolymers are investigated and discussed in relation to a conventional batch emulsion copolymerization model. The role of the surfactant in the ultrasonically initiated miniemulsion process is discussed.

[†] The University of Melbourne.
[‡] Wacker Chemicals Australia.
[§] Max-Planck Institute for Colloids and Interfaces.
* Author for correspondence.

10.1021/ma0473622 CCC: $30.25
Published on Web 06/18/2005

Experimental Section

Reagents. Methyl methacrylate (MMA, Aldrich, 99% (GC)) and butyl acrylate (BA, Fluka, purum >99% (GC)) were distilled under reduced pressure to remove inhibitor; the sealed purified samples were stored at 4 °C and kept in the dark until required. Sodium dodecyl sulfate (SDS, Fluka >98% GC), argon (BOC high purity grade), and tetrahydrofuran (THF, Fluka >99.5% GC) were used as supplied. Aqueous solutions were prepared with distilled water.

Copolymerization Method. All of the ultrasonically initiated miniemulsion copolymerization reactions reported here were performed as batch reactions using a conventional 19 mm diameter 20 kHz horn sonifier (Branson 450), using a previously described apparatus;[10] 20 kHz insonation is used as pyrolysis of organic compounds is negligible at 20 kHz compared to higher frequencies.[16,17] The power generated at the tip of the horn and absorbed by the solution was measured by calorimetry to lie between 7 and 9 W cm^{-2}. For all the batch polymerizations reported here, the concentration of monomer was 10 wt % in water and the SDS concentration was 25 mM (0.7 wt %). Monomer ratios are specified here as weight ratios.

The following description for a batch miniemulsion copolymerization at the above monomer concentration is typical of all the polymerizations described in this study. A mixture of monomer (7.5 g total), SDS (0.5 g), and water (67.5 g) was purged with argon for 45 min in the reaction vessel at room temperature. Thereafter, the argon gas stream was removed from the emulsion and was allowed to pass over the surface of the liquid mixture. The polymerization reaction was then initiated by subjecting this mixture to cycles of continuous sonication for 10 min, with 5 min pauses between sonication periods. This periodic sonication cycle and the immersion of the reaction vessel in an ice/water bath were sufficient to maintain the temperature at 25 ± 5 °C.

Gas Chromatography. Qualitative analysis of organic volatiles was performed by headspace autosampling coupled with a gas chromatograph and mass selective detector (Hewlett-Packard 5890 GC and 5971 MSD with a Perkin-Elmer HS40 headspace sampler). Analysis for pyrolysis products (methane, ethene, and ethyne) was also undertaken using gas chromatography (Shimadzu GC-17A) of the headspace following sonication of a sealed, argon-saturated monomer-in-water solution.

Polymer Conversion. Conversion data were obtained by gravimetry. Small amounts, <1%, of aggregated latex were formed around the horn; with coagulum taken into account, the overall conversion of monomer as measured by gravimetry at the end of sonication was ~90%. Free monomer analysis (by gas chromatography) on the final latex samples showed that there was no monomer left at the completion of the polymerizations, and it was determined that a negligible amount of monomer was lost by evaporation during the course of the reaction. While pyrolysis is minimized through the use of 20 kHz radiation,[16,17] due to the long time scales over which polymerization takes place, significant amounts of pyrolysis products (including[5] methane, ethane, and ethene, among other unidentified products) were observed by headspace analysis in this study.

Particle Sizing. Particle sizes were measured using a Nicomp submicron particle sizer (model 370). The latex dispersion was diluted by ~100 times with distilled water, with the monomer being sufficiently water-soluble that the unswollen particle size was measured. The measurements were carried out at 25 °C at a fixed scattering angle of 90°.

Molecular Weight Determination. Samples of dried latex were dissolved in toluene (HPLC grade, BDH) and passed through a 0.2 μm filter (Acrodisc, Gelman Laboratory). Light scattering measurements were undertaken using a DAWN DSP (Wyatt Technology) and calibrated against pMMA standards. For each sample, the weight-average molecular weight, $\bar{M}_w$, was determined using Zimm plots at five different concentrations of polymer.

Peroxide Yield. The radical yield of the ultrasound field in the absence of monomer and surfactant was quantified spectroscopically using standard techniques (absorption of the I_3^- ion at 352 nm).[18] The radical yield is estimated to be 4 times the peroxide yield, as two HO• radicals are required to form hydrogen peroxide, while two H• radicals will also be formed. From previous radical capture studies, the efficiency of initiation may be estimated as being ~20%.[19] Below, this is compared to initiation by the commonly used persulfate initiator (e.g., potassium persulfate, KPS), using appropriate Arrhenius parameters[20] and an appropriate entry efficiency model.[21]

Table 1. Parameters Used in the TRISEPS Program

parameter		value
reactivity ratios[a]	r_{MMA}	2.55
	r_{BA}	0.36
water solubility[b]	$[MMA]_{aq}^{sat}$	0.15 mol L^{-1}
	$[BA]_{aq}^{sat}$	0.01 mol L^{-1}
solubility in polymer	$[MMA]_p^{sat}$	6.0 mol L^{-1}
	$[BA]_p^{sat}$	5.5 mol L^{-1}

[a] Taken from ref 23. [b] Taken from ref 24.

Glass Transition Temperature. A small aliquot of the final latex solution was dissolved in THF (~1 mL), then precipitated in water (~10 mL), and dried. Measurements on the dried latex samples were performed using differential scanning calorimetry (DSC, Netzsch DSC 200) in an air atmosphere.

Copolymer Composition. The SDS was removed from the dried latex samples used for monomer conversion by dissolving the dried latex in a small aliquot of THF (~1 mL) and precipitating out the polymer with water (~10 mL). The solution was then filtered to collect the polymer and further rinsed with distilled water and then dried. These samples were used for copolymer composition analysis. The copolymer composition was determined by proton nuclear magnetic resonance (^{1}H NMR) using a Bruker DPX400 spectrometer. The samples were prepared in deuterated chloroform.

Model of Copolymer Composition. Simulations of the copolymer composition were performed using the computer model TRISEPS (Trimonomeric Seeded Emulsion Polymerization Simulation[22]). The model can predict the course of composition drift in seeded batch and semicontinuous emulsion co- and terpolymerizations of low to moderately water-soluble monomers. The model cannot predict particle nucleation, the overall rate of polymerization, or molecular weight distributions.

In TRISEPS, the terminal model for propagation is used, where it is assumed that the rate coefficient for propagation is dependent only on the identity of the terminal unit on the growing radical (and not on the penultimate unit). The propensity for a radical to add a like monomer compared to the other monomer in a copolymerization (the reactivity ratio, r), is used as a kinetic parameter in modeling such systems. For monomers M_A and M_B, one has $r_A = k_p^{AA}/k_p^{AB}$ and $r_B = k_p^{BB}/k_p^{BA}$, where k_p^{ij} is the second-order propagation rate coefficient for the reaction of a terminal radical derived from monomer i with monomer j.[22] The data used in the simulations reported here are shown in Table 1.

In this model, monomer partitioning (with the subscripts "d" and "p" denoting the droplet and particle concentrations, respectively) is described by the simplified equations derived by Maxwell et al.[25] and Noël et al.[26] for dispersed-phase polymerizations of one or more monomers. TRISEPS is not directly suited to modeling polymerizations involving droplet nucleation (where $[M]_p > [M]_p^{sat}$ during the first part of the reaction); however, as was shown by Maxwell et al.[25] that $[MA]_p^{sat}/[MB]_p^{sat} = [MA]_d^{sat}/[MB]_d^{sat}$, one can conclude that the ratio $[M_A]_p/[M_B]_p$ for a miniemulsion polymerization is correctly calculated by TRISEPS. Since it is this ratio (and the reactivity ratios) that determine the copolymer composition, one need only consider the influence of aqueous phase monomer to assess the applicability of TRISEPS to these miniemulsion polymerizations; it was shown by Schoonbrood et al.[22] that the

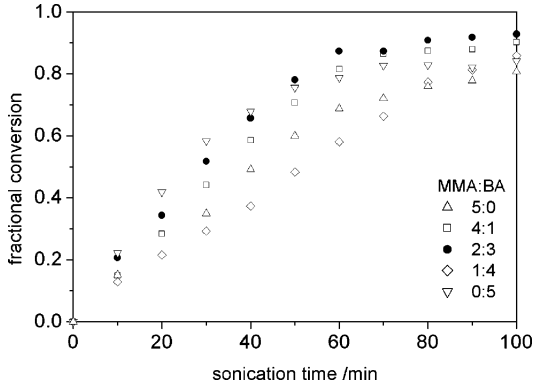

Figure 1. Total conversion (±4%) as a function of sonication time at 20 kHz under argon.

water solubility of the monomers had only a minor influence on the composition.

An upper bound to the sensitivity of the polymer composition to the difference between the emulsion and miniemulsion mechanism may be estimated using a "bootstrapping" approach where two TRISEPS simulations are combined, as follows. The first simulation using a recipe with negligible seed polymer is used to determine the composition of the polymer made at $t = 0$, which (as an upper bound) is assumed to be a constant composition for $[M]_p > [M]_p^{sat}$; the second simulation, with an amount of seed polymer included such that $[M]_p = [M]_p^{sat}$, is used to simulate the composition for higher conversions. The actual composition is calculated from these two simulations by mass balance; the composition so calculated differs from a naive application of the TRISEPS model to these recipes by a maximum of 3.6% (at $[M]_p = [M]_p^{sat}$) and by less than 0.6% at 80% conversion. We therefore conclude that the application of the TRISEPS model to miniemulsion copolymerizations is justified.

Results and Discussion

Conversion Profiles and Particle Size. Recipes with monomer compositions based on weight ratios of 0:5, 4:1, 2:3, 1:4, and 5:0 MMA/BA (with a total monomer fraction of 10 wt % in the emulsion) were studied at constant monomer fraction and surfactant concentration to investigate the effect of monomer composition on conversion profiles and particle size. The conversion−sonication time curves are presented in Figure 1. The conversion profiles at each comonomer composition are comparable.

During an ultrasonically initiated miniemulsion polymerization a droplet nucleation mechanism is operative, as follows.[9] Primary radicals produced within cavitation bubbles during insonation may then add to either adsorbed or aqueous monomer, forming monomeric-adduct radicals (HM$^\bullet$ and HOM$^\bullet$). Droplets of monomer in the miniemulsion size range (50−500 nm, produced by the continuous shearing generated by acoustic bubble collapse[7,27]) are polymerized following reaction with these monomeric-adduct radicals. Figure 2 pictorially describes these events. It may be reasonably established that micellar nucleation is negligible using the simple surfactant coverage model of Giannetti:[28] using the experimentally determined droplet size for ultrasonic shearing,[29] the surface area of the droplets is sufficiently large that the surfactant coverage is only 70% of the maximum value obtainable using appropriate values for the surface area per surfactant on polymer particles;[30] hence, micelles are not present in the system.

The periodic measurement of the concentration hydrogen peroxide over the course of 1 h of sonication gave a radical yield of 1.3×10^{-7} mol dm^{-3} s^{-1}. Across a population of particles at $N_p = 1.0 \times 10^{18}$ dm^{-3} and an estimated radical entry efficiency of 20%,[19] this gives an radical entry frequency, $\rho = 1.5 \times 10^{-2}$ s^{-1} (one radical entry per particle every 65 s). For the purposes of comparison, the radical entry frequency of 3.0 mmol dm^{-3} KPS at 25 °C is 6.2×10^{-5} s^{-1} (which is lower than the usual level of spontaneous initiation[21]) and at 50 °C is 3.2×10^{-3} s^{-1}. Thus, the radical yield of water-derived radicals from insonation is sufficiently high that thermal initiation in the system is insignificant. Similarly, the direct formation of initiating radicals from monomer during ultrasonic cavitation is negligible, since the monomer is present in the bulk liquid in only low concentrations; recently reported pyrolysis studies show that pyrolysis of organic compounds is considerably lower at 20 kHz compared to higher frequencies.[16,17]

The particle diameter as a function of sonication time is shown in Figure 3. It may be noted that the particle size is relatively unaffected by the comonomer composition, owing to the high-shear, high-flow environment that is created by the ultrasonic field; this is consistent with recently reported freeze-fracture electron microscopy experiments that show that the (initial) droplet size in an ultrasonic field is a kinetic (not thermodynamic) phenomenon and is independent of the oil being dispersed for a wide range of hydrocarbons.[29] The polymers with the highest proportion of MMA have a constant particle diameter as a function of sonication time, whereas with increased amounts of BA in the initial comonomer the particle diameter increased with sonication time.

Figure 4 shows the corresponding dependence of the particle number on sonication time; for the purposes of comparison of the trends in particle number, the particle number relative to the final particle number is shown in Figure 4b, and it is this representation of the data that we will now discuss in detail. Note that the observed increases in particle number are due to the nucleation of new particles, while the observed decreases in particle number can only be explained by particle−particle coalescence. Figure 4b shows that the particle number for all copolymer compositions was observed to increase for the first 30 min of sonication

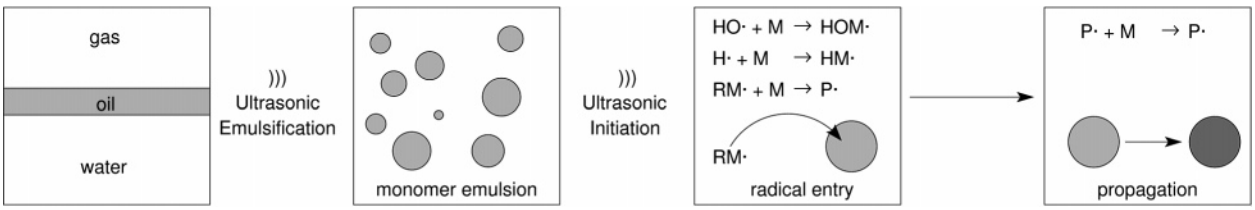

Figure 2. Schematic of the miniemulsion mechanism proposed to be operative during ultrasonically initiated emulsion polymerization. The ultrasonic field is used to maintain a small monomer droplet size as well as to generate $^\bullet$OH and H$^\bullet$ radicals to initiate polymerization. Particle formation is by droplet nucleation.

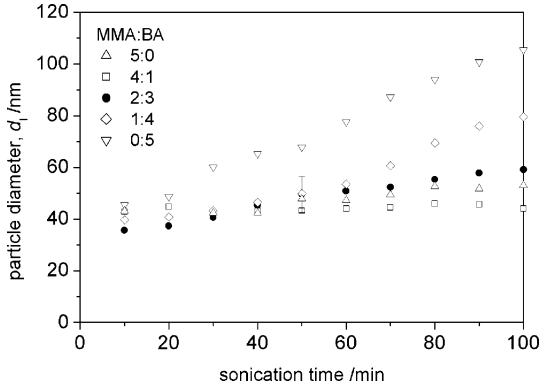

Figure 3. Intensity average particle diameter as a function of sonication time for the comonomer compositions studied. The indicated uncertainty is the systematic error range associated with all data points.

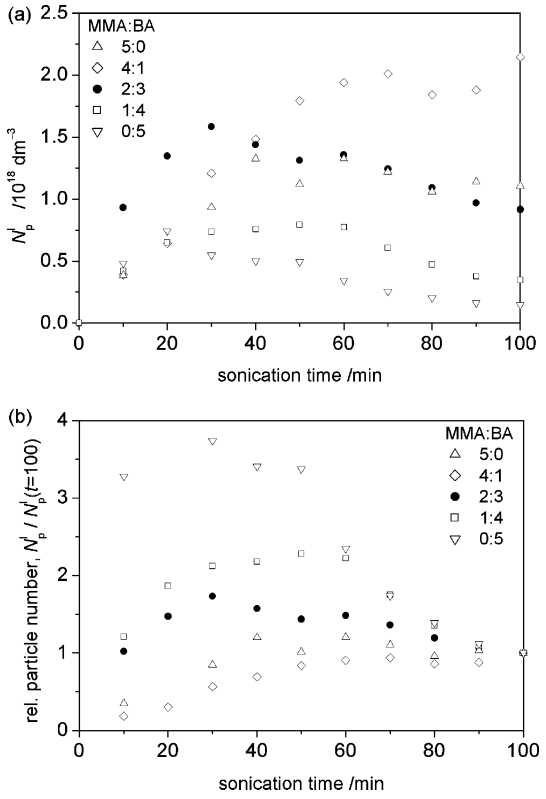

Figure 4. Evolution of the particle number (N_p^I, calculated from $\langle d_I \rangle$) in the reaction: (a) particle number concentration and (b) the number of particles in each reaction relative to the number at the end of the reaction.

during the period of initial droplet nucleation. With further sonication, the MMA-rich polymerizations continue on this trend up to 70 min of sonication, after which the particle number remained approximately constant. For the other polymers, the particle number decreased with continued sonication; since the mixture is constantly being sheared by ultrasound-induced cavitation, the mechanical properties of the droplets and particles involved in collision events are significant in interpreting the trends shown in Figure 4b.

Further consideration of Figure 4b shows that the particle number in this system is correlated to the glass transition temperature (T_g) of the polymers formed, providing additional evidence for our previous postulate;[9] over a range of copolymer compositions, the polymers with higher T_g have increasing particle number throughout the polymerization, while the lower T_g polymers have a decreasing particle number from ~40% conversion. At longer sonication times (higher conversion) the number of particles increases until [particles]/[droplets] > ~1, and the rate of particle−particle collisions increases. However, rubbery particles are more likely to coalesce during collision than are glassy polymers, while particle-droplet coalescence may be undone either by subsequent ultrasonic shear or by monomer diffusion. One may now recast the above explanation of Figure 4b in terms of the mechanical properties of the polymers. For the first ~40 min of sonication, droplet−droplet interactions dominate, and the trend in the particle number for all compositions is similar. After that time the droplet−particle and particle−particle interactions in the high-T_g systems do little to change the particle number, although droplet nucleation continues until ~70 min of sonication; the low-T_g systems show significant amounts of particle−particle coalescence after this time.

Table 2. Molecular Weight and Calculated Kinetic Chain Length

system	measured $\bar{M}_w$	kinetic chain length
MMA	3.6×10^6	1.8×10^7
BA	4.8×10^6	3.1×10^6

The experimentally determined weight-average molecular weights of the MMA and BA polymerizations are shown in Table 2, along with the calculated kinetic chain length data. The measured molecular weights for the MMA and BA systems are quite similar; however, the measured molecular weight for the MMA system is considerably less than the kinetic chain length, while these values are comparable for BA. Since small MMA particles with the high radical flux calculated above would be described by zero−one kinetics,[31] the chain length may crudely be estimated from the period between radical entry events as $v_{entry} = M_{MMA}k_p/\rho$, where M_{MMA} is the molecular weight of the MMA monomer (a more detailed description using zero−one−two kinetics is also possible[32]). The entry-determined molecular weight, 2.1×10^6, compares quite favorably to the experimentally determined molecular weight.

Surfactant in Miniemulsion Processes. It has been hypothesized by other workers that the surfactant is responsible for initiation in the ultrasonically initiated miniemulsion polymerization of various monomers, including MMA[33] and BA,[34] being described as "one of the radical sources".[34] Such conclusions were based upon the comparison of conversion−time data both with and without added surfactant; in the absence of surfactant, little conversion was obtained, while with surfactant quite rapid conversion was observed.

However, such a conclusion neglects three important aspects of the ultrasonically initiated system. First, the aqueous concentration of surfactant is limited by its cmc (i.e., [SDS] < 8 mM), but the monomer is frequently in much greater concentration ($[MMA]_{aq} \approx 0.15$ M); since addition to monomer and abstraction of hydrogen from SDS have similar second-order rate coefficients, it is kinetically unlikely that the surfactant is involved in the radical chemistry. Second, it is well-known that the reaction rate of emulsion and miniemulsion polymerizations is dependent on the number of particles in which the polymerization is taking place.[35] Since the number of droplets is dependent on the stabilizers used,[36] and miniemulsion polymerization implies a droplet nucle-

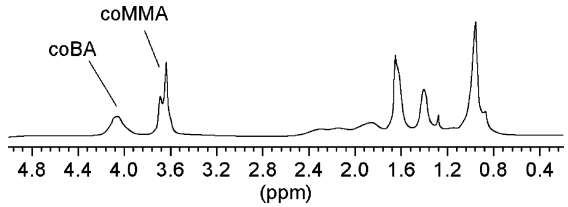

Figure 5. NMR spectra of fully converted 2:3 poly(MMA-*co*-BA). The peak labeled coBA relates to the resonance of the OCH_2 protons of BA and that labeled coMMA to the resonance of the OCH_3 protons of MMA. The integral of these peaks was used to calculate the ratio of each monomer in the copolymer.

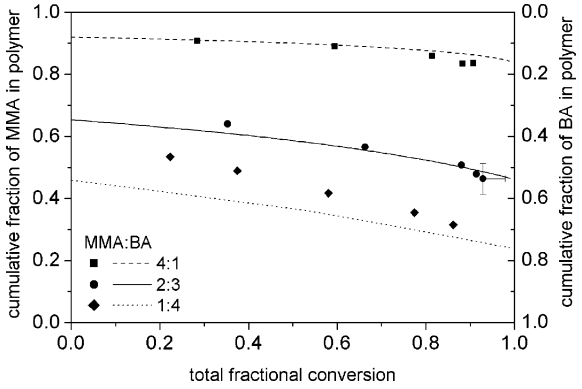

Figure 6. Cumulative fraction of MMA and BA in the formed copolymer as a function of the overall conversion for various MMA:BA comonomer compositions. Experimental data are shown as points; TRISEPS modeling results are shown as lines.

ation process,[7] the rate of polymerization will be strongly influenced by the nature and concentration of the surfactant (particularly toward the limiting case of no surfactant), without it being involved in the free-radical chemistry. Finally, in the study of the miniemulsion polymerization of MMA by ultrasound, it was found that the surfactant used to stabilize the monomer droplets could be completely removed by dialysis after polymerization was complete. This indicates that no covalent bonding of the surfactant to the polymer had taken place.[9]

Copolymer Composition. The results so far do not suggest a significant deviation from the classical mechanism of free-radical copolymerization. However, our interest lies in investigating whether the composition of polymers formed is consistent with this technique. The physical properties of copolymers depend on the nature of the monomers as well as the copolymer composition and the compositional drift; the resulting particle structure may have a different morphological complexity to the films cast from them.

A typical ^1H NMR spectrum is shown in Figure 5 for the 2:3 reaction to form poly(MMA-*co*-BA). The cumulative monomer fraction and partial conversion vs the overall conversion are plotted in Figures 6 and 7, respectively. In these figures, the solid lines give the compositions predicted using TRISEPS. For all monomer ratios at low conversions, the proportion of MMA in the polymer is higher than the proportion of monomer in the recipe. This is because the MMA is preferentially incorporated, with both MMA terminal radicals and BA terminal radicals being more likely to add to MMA (i.e., $r_{MMA} > 1 > r_{BA}$). With increasing conversion, the cumulative ratio of MMA in the formed copolymer decreases, approaching the ratio in the original recipe. The compositional trends for ultrasonically synthesized

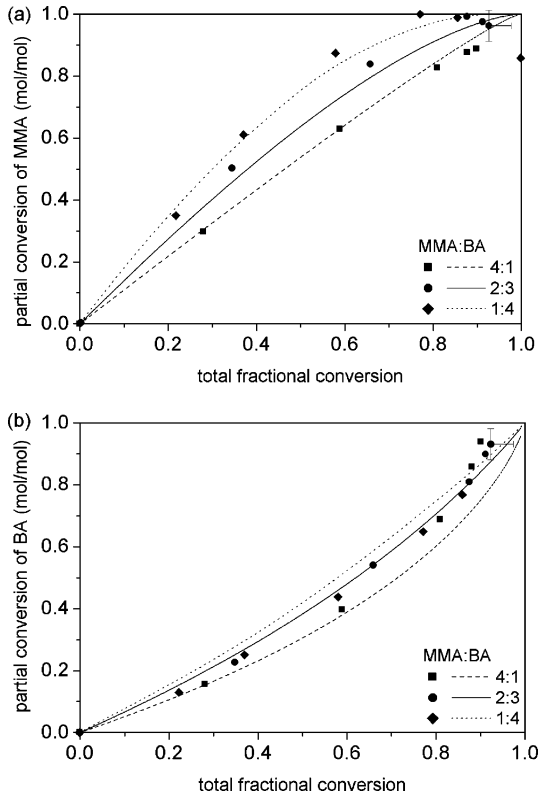

Figure 7. Experimentally determined (points) and TRISEPS modeling (lines) of the partial conversion of (a) MMA and (b) BA vs the overall conversion for various MMA:BA comonomer compositions.

Table 3. MMA:BA Copolymer Glass Transition Data

comonomer composition (MMA:BA)	T_g(DSC)/(±20), °C
5:0	+110
4:1	+90
2:3	+60
1:4	−10 and +50
0:5	−40

copolymers are consistent with conventional composition (shown by the theoretical curves), where at constant water:monomer ratio the compositional drift is mainly determined by the reactivity ratios.[37]

Whereas differences between the predicted and observed compositional trends are seen, they are within the uncertainty of the model (stated earlier) and the experimental data (shown in Figure 7). A significant source of error in these measurements is related to difficulties in accurately estimating the conversion during ultrasonic synthesis due to degradation of some monomer and limited coagulation on the sonic horn.[9] In addition, there is reasonable variation in the values of the reactivity ratios, which accounts for a small variation in the predicted composition.[23] The agreement between the experimental trends and the predictions are within the bounds of these uncertainties, such that an effect of ultrasound on the specificity of the terminal radicals for the comonomers (i.e., the reactivity ratios) cannot be identified.

Data for the T_g of the sonochemically produced polymers are shown in Table 3 for a variety of comonomer ratios. The observed T_g's for the sonochemically produced copolymers are between those of the two homopolymers; as the mole fraction of BA increases in the copolymer, T_g trends toward lower values. In the

case of the 2:3 and 4:1 (MMA:BA) compositions, these data indicate that a copolymer is formed (not a polymer blend), and compositional drift during the course of the polymerization has minimal effect on the physical properties of the polymer.

In the BA-rich copolymer, two glass transitions are observed. This may be understood as resulting from a sufficiently large compositional drift throughout the course of the reaction such that the chains produced are not mutually compatible and demixing occurs into two phases[38] (noting that the compositional drift occurs between different chains and not along the same chain as would be seen in a living polymerization[39]). The specificity of both terminal radicals for MMA leads to rapid depletion of MMA in this BA-rich recipe, leading to two polymer phases, one consisting of polymers relatively rich in MMA and the other of polymer very rich in BA; this effect is accentuated by the differing water solubilities of the two monomers.[22] These phases have a different T_g, as seen in Table 3.

Conclusions

The copolymer compositions observed during an ultrasonically initiated emulsion polymerization indicate that the terminal model can adequately describe the copolymer composition. The results obtained from an analysis of the glass transition temperatures suggest that true copolymers are formed, with a microstructure similar to that which can be obtained in a classical copolymerization initiated with chemical free-radical sources. This is indicative of the case that ultrasound has little effect on the propagation step of a free-radical polymerization process, making ultrasound a useful source of free radicals to initiate dispersed-phase polymerizations. The particle size data, along with previous incorporation studies,[40] suggest that ultrasonically initiated emulsion polymerization occurs by a miniemulsion polymerization process, giving rapid rates of conversion and indicating that the role of the surfactant in the polymerization is purely in particle stabilization and not in free-radical chemistry.

Acknowledgment. M.A.B. acknowledges the receipt of an Australian Postgraduate Award. The project was in part funded by Dulux Australia Pty. Ltd. and the ARC Particulate Fluids Processing Centre and the Max Planck Institute of Colloids and Interfaces (Golm).

References and Notes

(1) Price, G. J. *Ultrason. Sonochem.* **1996**, *3*, S229−S238.
(2) Landfester, K. *Macromol. Rapid Commun.* **2001**, *22*, 896−936.
(3) Anderson, C. D.; Sudol, E. D.; El-Aasser, M. S. *Macromolecules* **2002**, *35*, 574−576.
(4) Didenko, Y. T.; McNamara III, W. B.; Suslick, K. S. *J. Am. Chem. Soc.* **1999**, *121*, 5817−5818.
(5) Tauber, A.; Mark, G.; Schuchman, H. P.; Sonntag, C. V. *J. Chem. Soc., Perkin Trans. 2* **1999**, 1129−1135.
(6) McAskill, N. A.; Sangster, D. F. *Aust. J. Chem.* **1979**, *32*, 2611−2615.
(7) Landfester, K.; Bechthold, N.; Forster, S.; Antonietti, M. *Macromol. Rapid Commun.* **1998**, *20*, 81−84.
(8) Pham, B. T. T.; Nguyen, D.; Ferguson, C. J.; Hawkett, B. S.; Serelis, A. K.; Such, C. H. *Macromolecules* **2003**, *36*, 8907−8909.
(9) Bradley, M. A.; Grieser, F. *J. Colloid Interface Sci.* **2002**, *251*, 78−84.
(10) Biggs, S.; Grieser, F. *Macromolecules* **1995**, *25*, 4877−4882.
(11) Ooi, S. K.; Biggs, S. *Ultrason. Sonochem.* **2000**, *7*, 125−133.
(12) Chou, H. C. J.; Stoffer, J. O. *J. Appl. Polym. Sci.* **1999**, *72*, 797−825.
(13) Liao, Y. Q.; Wang, Q.; Wang, L. W. *Chem. J. Chin. Univ.* **2002**, *23*, 2192−2195.
(14) Cooper, G.; Grieser, F.; Biggs, S. *J. Colloid Interface Sci.* **1996**, *184*, 52−63.
(15) Walton, A. J.; Reynolds, G. T. *Adv. Phys.* **1984**, *33*, 595−660.
(16) Tronson, R.; Ashokkumar, M.; Grieser, F. *J. Phys. Chem. B* **2002**, *106*, 11064−11068.
(17) Price, G. J.; Ashokkumar, M.; Grieser, F. *J. Am. Chem. Soc.* **2004**, *126*, 2755−2762.
(18) Hochanadel, C. J. *J. Phys. Chem.* **1952**, *56*, 587−594.
(19) Fischer, C.-H.; Hart, E. J.; Henglein, A. *J. Phys. Chem.* **1986**, *90*, 222−224.
(20) Behrman, E. J.; Edwards, J. O. *Rev. Inorg. Chem.* **1980**, *2*, 179.
(21) van Berkel, K. Y.; Russell, G. T.; Gilbert, R. G. *Macromolecules* **2003**, *36*, 3921−3931.
(22) Schoonbrood, H. A. S.; Eijnatten, R. C. P. M.; van den Reijen, B.; van Herk, A. M.; German, A. L. *J. Polym. Sci., Part A: Polym. Chem.* **1996**, *34*, 935−947.
(23) Buback, M.; Felderman, A.; Barner-Kowollik, C.; Lacík, I. *Macromolecules* **2001**, *34*, 5439−5448.
(24) Napper, D. H.; Gilbert, R. G. In *Comprehensive Polymer Science*; Allen, G. A.,Bevington, J. C., Eastmond, G. C., Eds.; Pergamon: Oxford, 1989; Vol. 4.
(25) Maxwell, I. A.; Kurja, J.; van Doremaele, G. H. J.; German, A. L.; Morrison, B. R. *Makromol. Chem.* **1992**, *193*, 2049−2063.
(26) Noël, L. F. J.; Maxwell, I. A.; German, A. L. *Macromolecules* **1993**, *26*, 2911−2918.
(27) Lovell, P. A.; El-Aasser, M. S. *Emulsion Polymerization and Emulsion Polymers*; John Wiley and Sons: Chichester, 1997.
(28) Giannetti, E. *AIChE J.* **1993**, *39*, 1210−1227.
(29) Sakai, T.; Kamogawa, K.; Harusawa, F.; Momozawa, N.; Sakai, H.; Abe, M. *Langmuir* **2001**, *17*, 255−259.
(30) Ahmed, S. M.; El-Aasser, M. S.; Micale, F. J.; Poehlein, G. W.; Vanderhoff, J. W. In *Polymer Colloids II*; Fitch, R. M., Ed.; Plenum: New York, 1980.
(31) Prescott, S. W.; Ballard, M. J.; Gilbert, R. G. *J. Polym. Sci., Part A: Polym. Chem.* **2005**, *43*, 1076−1089.
(32) Napper, D. H.; Lichti, G.; Gilbert, R. G. In *Emulsion Polymers and Emulsion Polymerization*; Bassett, D. R., Hamielec, A. E., Eds.; ACS Symposium Series Vol. 165; American Chemical Society: Washington, DC, 1981.
(33) Liao, Y. Q.; Wang, Q.; Xia, H. S.; Xu, X.; Baxter, S. M.; Slone, R. V.; Wu, S. G.; Swift, G.; Westmoreland, D. G. *J. Polym. Sci., Part A: Polym. Chem.* **2001**, *39*, 3356−3364.
(34) Xia, H. S.; Wang, Q.; Liao, Y. Q.; Xu, X.; Baxter, S. M.; Slone, R. V.; Wu, S. G.; Swift, G.; Westmoreland, D. G. *Ultrason. Sonochem.* **2002**, *9*, 151−158.
(35) Gilbert, R. G. *Emulsion Polymerization: A Mechanistic Approach*; Academic: London, 1995.
(36) Miller, C. M.; Venkatasan, J.; Silebi, C. A.; Sudol, E. D.; El-Aasser, M. S. *J. Colloid Interface Sci.* **1994**, *162*, 11−18.
(37) Wu, X. Q.; Schork, F. J. *Ind. Eng. Chem. Res.* **2000**, *39*, 2855−2865.
(38) Fernandez-Garcia, M.; Cuervo-Rodriguez, R.; Madruga, E. L. *J. Polym. Sci., Part B: Polym. Phys.* **1999**, *37*, 2512−2520.
(39) Prescott, S. W.; Ballard, M. J.; Rizzardo, E.; Gilbert, R. G. *Aust. J. Chem.* **2002**, *55*, 415−424.
(40) Bradley, M. A.; Ashokkumar, M.; Grieser, F. *J. Am. Chem. Soc.* **2003**, *125*, 525−529.

MA0473622